Biochimica et Biophysica Acta 1838 (2014) 747–755

Contents lists available at ScienceDirect

Biochimica et Biophysica Acta

journal homepage: www.elsevier.com/locate/bbamem

Multiple cysteine residues are necessary for sorting and transport activity of the arsenite permease Acr3p from *Saccharomyces cerevisiae*

Ewa Maciaszczyk-Dziubinska, Magdalena Migocka, Donata Wawrzycka, Katarzyna Markowska, Robert Wysocki *

Institute of Experimental Biology, University of Wroclaw, 50-328 Wroclaw, Poland

ARTICLE INFO

Article history:
Received 18 July 2013
Received in revised form 13 November 2013
Accepted 20 November 2013
Available online 28 November 2013

Keywords:
Yeast
Arsenite transporter
Mutagenesis
Plasma membrane
Acr3 permease

ABSTRACT

The yeast transporter Acr3p is a low affinity As(III)/H^+ and Sb(III)/H^+ antiporter located in the plasma membrane. It has been shown for bacterial Acr3 proteins that just a single cysteine residue, which is located in the middle of the fourth transmembrane region and conserved in all members of the Acr3 family, is essential for As(III) transport activity. Here, we report a systematic mutational analysis of all nine cysteine residues present in the *Saccharomyces cerevisiae* Acr3p. We found that mutagenesis of highly conserved Cys151 resulted in a complete loss of metalloid transport function. In addition, lack of Cys90 and Cys169, which are conserved in eukaryotic members of Acr3 family, impaired Acr3p trafficking to the plasma membrane and greatly reduced As(III) efflux, respectively. Mutagenesis of five other cysteines in Acr3p resulted in moderate reduction of As(III) transport capacities and sorting perturbations. Our data suggest that interaction of As(III) with multiple thiol groups in the yeast Acr3p may facilitate As(III) translocation across the plasma membrane.

1. Introduction

Arsenic is a highly toxic metalloid and human carcinogen which is commonly found in the environment from both geological and anthropogenic sources [1–3]. Thus, it is crucial to develop biological strategies to avoid accumulation of arsenic in crops and prevent arsenic poisoning in humans as well as to decontaminate polluted areas. On the other hand, arsenic displays an antitumor activity and is one of the most effective drugs in the treatment of acute promyelocytic leukemia with a clinical potential to cure other types of cancer and autoimmune diseases [4–6]. Compounds containing the related metalloid antimony remain the first line drugs against leishmaniasis [7]. Understanding of molecular mechanisms of arsenic and antimony transport in various organisms is necessary to cope with emerging resistance to metalloid-based drugs and to generate new plant species with low or increased ability to accumulate arsenicals and antimonials.

The Acr3 family of arsenite (As(III)) transporters, belonging to the bile/arsenite/riboflavin transporter (BART) superfamily [8], is the major detoxification system for arsenic in both prokaryotes and eukaryotes [9,10]. The Acr3 transporters are widespread in bacteria, archaea, fungi and lower plants [11–14]. Although the Acr3 orthologs have not been found in the genomes of flowering plants, heterologous expression of the yeast *ACR3* gene in rice and *Arabidopsis thaliana* significantly improved tolerance to As(III) by reducing its accumulation in transgenic plants [15,16]. Our genome database searches have identified new eukaryotic members of the *ACR3* gene family in chlorophyta (*Coccomyxa subellipsoidea*), slime mold (*Polysphondylium pallidum*), heterokonts (*Phytophthora infestans*) and choanoflagellates (*Monosiga brevicollis*) (Fig. 1A).

The Acr3 permeases have ten-transmembrane span topology [11,17] and usually localize to the plasma membrane to mediate As(III) efflux and confer high-level resistance to this toxic metalloid in *Bacillus subtilis* [18], *Alkaliphilus metalliredigens*, *Corynebacterium glutamicum* [11], and *Saccharomyces cerevisiae* [19–21]. In the arsenic hyperaccumulating fern *Pteris vittata* Acr3 is targeted to the vacuolar membrane to sequestrate As(III) into the intracellular compartment instead of extrusion out of the cell [14]. The *Shewanella oneidensis* Acr3 is not able to transport As(III) and confers resistance only to arsenate (As(V)) [22], while the Acr3 ortholog from *Synechocystis* sp. mediates tolerance to As(III), As(V) and antimonite (Sb(III)) [23]. Recently, we have shown that the *S. cerevisiae* Acr3p is also able to extrude Sb(III) but confers only a moderate level of Sb(III) resistance [21]. Consistently, we have provided in vitro evidence that Acr3p catalyzes low affinity As(III)/H^+ and Sb(III)/H^+ antiport coupled to the proton-motive force but the rate of Sb(III) transport is much slower compared to As(III) [24]. However, the involvement of particular amino acid residues in As(III) and Sb(III) translocation via the *S. cerevisiae* permease Acr3p has not been investigated yet.

It has been determined that the mutagenesis of single cysteine residue in the *C. glutamicum* (Cys129) and *A. metalliredigens* Acr3 (Cys138),

Abbreviations: As(III), arsenite; As(V), arsenate; Sb(III), antimonite; ER, endoplasmic reticulum; TM, transmembrane segment

* Corresponding author at: Institute of Experimental Biology, University of Wroclaw, Kanonia 6/8, 50-328 Wroclaw, Poland. Tel.: +48 71 375 4126; fax: +48 71 375 4118.
E-mail address: robert.wysocki@biol.uni.wroc.pl (R. Wysocki).

0005-2736/$ – see front matter © 2013 Elsevier B.V. All rights reserved.
http://dx.doi.org/10.1016/j.bbamem.2013.11.013

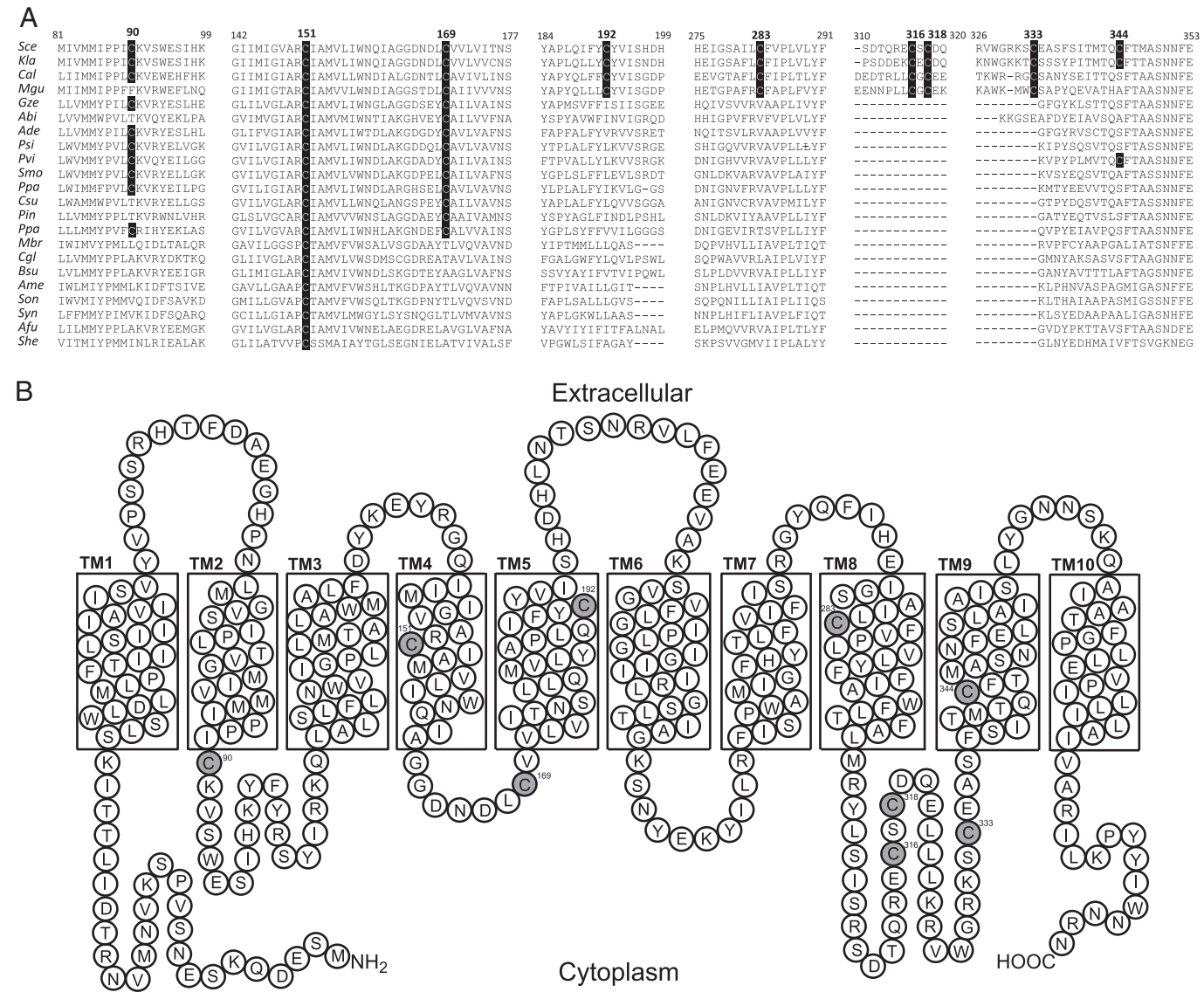

Fig. 1. Conservation of cysteine residues in the Acr3 family and hypothetical topology model of the Acr3 plasma membrane protein from *S. cerevisiae*. (A) Alignment of protein sequences of Acr3 orthologs was performed with Clustal Omega (http://www.ebi.ac.uk/Tools/msa/clustalo) [30]. The alignment includes representative eukaryotic members of the Acr3 family from fungi (Ascomycota and Basidiomycota), vascular plants (spikemoss, fern and spruce), Bryophyta (moss), Chlorophyta (green algae), Stramenopiles (heterokonts), Amebozoa (slime mold) and Choanoflagellida (choanoflagellates) as well as a few examples of prokaryotic Acr3 proteins from gram positive and gram negative bacteria and archaea (Euryarchaeota and Crenarchaeota). The following protein sequences of Acr3 family members obtained from NCBI (accession numbers in parentheses) were used in the alignment: *Saccharomyces cerevisiae* S288c (Sce, DAA11615), *Kluyveromyces lactis* NRRL Y-1140 (Kla, XP_455090), *Candida albicans* SC5314 (Cal, XP_715501), *Meyerozyma guilliermondii* ATCC 6260 (Mgu, XP_001481996), *Gibberella zeae* PH-1 (Gze, XP_386755), *Agaricus bisporus* var. *burnettii* JB137-S8 (Abi, EKM76040), *Auricularia delicata* TFB-10046 SS5 (Ade, EJD54751), *Picea sitchensis* (Psi, ADE76924), *Pteris vittata* (Pvi, ADP20955), *Selaginella moellendorffii* (Smo, XP_002970839), *Physcomitrella patens* subsp. *patens* (Ppa, YP_001138464), *Coccomyxa subellipsoidea* C-169 (Csu, EIE24472), *Phytophthora infestans* T30-4 (Pin, EEY55020), *Polysphondylium pallidum* PN500 (Ppa, EFA79047), *Monosiga brevicollis* MX1 (Mbr, EDQ91878), *Corynebacterium glutamicum* ATCC 13032 (Cgl, YP_225795), *Bacillus subtilis* (Bsu, BAA12433), *Alkaliphilus metalliredigens* QYMF (Ame, YP_001319657), *Shewanella oneidensis* MR-1 (Son, AAN53615), *Synechocystis* sp. PCC 6803 (Syn, BAA18405), *Archaeoglobus fulgidus* DSM 4304 (Afu, AAB90761), and *Staphylothermus hellenicus* DSM 12710 (She, YP_003668173). For simplicity, only fragments of protein sequences containing conserved cysteine residues are shown. The conserved cysteine residues are highlighted. Sequence coordinates are from the *S. cerevisiae* Acr3p. (B) The transmembrane topology of Acr3p was predicted by the HMMTOP method (http://www.enzim.hu/hmmtop) [29], which best fits the Acr3 topology determined for bacterial species [11,17,25]. Cysteine residues subjected to mutagenesis are in gray circles.

located in the middle of the fourth transmembrane domain and conserved in all members of the Acr3 family, resulted in a complete loss of transport activity [11,25]. This suggests that interaction of As(III) with a single thiol group is required to activate As(III) transport capacity of bacterial Acr3 proteins. In addition, a conserved glutamate (Glu305) in the *C. glutamicum* Acr3 has been proposed to be involved in H^+ translocation [25]. Here, we analyzed the effect of mutagenesis of nine cysteine residues present in the yeast permease Acr3p and found that lack of Cys151, which corresponds to Cys129 in the *C. glutamicum* Acr3 and Cys138 in the *A. metalliredigens* Acr3, also completely abolished the ability of the *S. cerevisiae* Acr3p to mediate As(III) efflux. In addition, we showed the importance of seven other cysteine residues for proper Acr3p trafficking to the plasma membrane as well as for its transport activity.

2. Materials and methods

2.1. Mutagenesis of ACR3 gene

The pUG35 plasmids (CEN, *URA3*, Amp^R) containing the *ACR3*-GFP fusion gene under the control of the native promoter (pACR3-GFP) [21] or the *MET25* promoter (pMET-ACR3-GFP) were used as templates

for site-directed mutagenesis with the QuikChange Lightning kit (Agilent Technologies) and confirmed by DNA sequencing. Cys90, Cys151, Cys169, Cys192, Cys283, Cys316, Cys318, Cys333 and Cys344 residues in the *S. cerevisiae* Acr3p were changed into alanines or valine using oligonucleotides listed in Supplementary Table S1.

2.2. Growth conditions

The *acr3Δ::kanMX* single mutant (RW104) in W303-1A background (*MATa ura3 leu2 trp1 his3 ade2 can1*) [26] was transformed with either an empty vector pUG35, pACR3-GFP, and pMET-ACR3-GFP or the plasmids bearing the mutated versions of *ACR3* gene. Yeast transformants were grown to mid-log phase in selective minimal medium lacking uracil (2% glucose, 0.67% yeast nitrogen base, supplemented with leucine, tryptophan, histidine and adenine) at 30 °C and plated on solid selective minimal media containing various concentrations of sodium arsenite, sodium arsenate or potassium antimonyl tartrate. Plates were photographed after 2–3 days at 30 °C. Growth assays were performed at least two times with different sets of transformants with similar results and representative data are shown. Alternatively, yeast transformants were exposed to 1 mM sodium arsenite in liquid minimal media for 36 h. The growth rate was determined by measuring optical density at 600 nm. For preparation of RNA, protein and microscopy analysis yeast transformants were grown to mid-log phase and exposed to 0.1 mM sodium arsenite for 4 h to induce expression of wild-type and mutated forms of Acr3-GFP protein.

2.3. Determination of intracellular As content

Exponentially growing cells were exposed to 0.1 mM As(III) for 2 h followed by 2 h incubation in the presence of 1 mM As(III). Next cell cultures were washed to remove As(III) from the medium, and resuspended in fresh medium to measure As(III) efflux. Culture samples were collected at 0 and 4 h time point after release, washed in ice-cold water and centrifuged. The cell pellets were resuspended in water, boiled for 10 min, and centrifuged to collect the supernatant. The As content of each sample was determined using a flame atomic absorption spectrometer (3300, Perkin Elmer).

2.4. RNA extraction, reverse transcription and quantitative PCR

In order to determine the level of mRNA for wild-type *ACR3* and cysteine mutants, total RNA was isolated from yeast transformants after exposure to 0.1 mM As(III) for 4 h using RNeasy Mini Kit (Qiagen). Reverse transcription was performed with 1.5 μg of purified RNA using High-Capacity cDNA Reverse Transcription Kit (Applied Biosystems) according to the manufacturer's directions. Real-time amplification was performed in LightCycler 480 System (Roche Applied Science) with the RealTime 2xPCRMaster Mix SYBR kit (A&A Biotechnology) according to the manufacturer's instructions using 1 μL of cDNA and the primers ACR3RT-F and ACR3RT-R (Supplementary Table S1) in a total volume of 20 μL. All results were standardized using the housekeeping gene *IPP1*, encoding for inorganic pyrophosphatase, with IPP1F and IPP1R primers (Supplementary Table S1). For each of the RNA extractions, measurements of gene expression were obtained in triplicate, and the mean of these values was used for further analysis. Measurements of *ACR3* mRNA levels were repeated three times and error bars indicate standard deviation (SD).

2.5. Protein extraction and immunoblotting

Total protein was extracted by the trichloroacetic acid method as described previously [27]. Protein extracts were resolved on 10% SDS-PAGE, blotted onto nitrocellulose filters (Bio-Rad) and probed with the anti-GFP antibody (Roche) to detect Acr3p tagged with a green fluorescent protein (GFP) and the anti-PSTAIRE antibody (Santa Cruz Biotechnology) to examine the level of cyclin-dependent kinases Cdc28p and Pho85p as a protein loading control.

2.6. Fluorescence microscopy

Distribution of GFP-tagged wild-type and mutant Acr3 proteins in live cells was examined with an Axio Imager M1 upright wide-field fluorescence microscope (Carl Zeiss, Germany) equipped with an illuminator (Zeiss HBO 100), a 100× oil immersion objective (Zeiss Plan-Neofluar 100x/1.30), and a GFP filter set. Images were collected using a Zeiss AxioCam MRc digital camera and processed with Zeiss AxioVision 4.5 software.

2.7. Isolation of plasma membrane vesicles

Plasma membranes were isolated essentially as described earlier [24,28] from yeast cells treated with 1 mM As(III) for 4 h to induce Acr3p expression. The everted plasma membrane vesicles were separated from total microsomes by partitioning in a two-phase system consisting of 6.2% dextran T-500 and 6.2% polyethylene glycol 3350. The orientation and purity of the final plasma membrane fraction was verified as described elsewhere [24]. Membrane vesicles were immediately used for transport assay or frozen at −80 °C until used for western blot analysis. Protein content was quantified using the Bio-Rad protein assay reagent with bovine serum albumin as a standard. Immunoblotting of the membrane-enriched protein fraction was performed with the anti-GFP antibody (Roche) to detect Acr3p or the anti-Pma1p antibody against the plasma membrane H^+-ATPase (kindly provided by M. Ghislain, University of Louvain, Belgium) as a quality control of isolated plasma membranes.

2.8. Transport assays in everted membrane vesicles

The absorbance change of acridine orange was used to monitor the formation and dissipation of inside-acid pH gradients across the plasma membrane vesicles. Purified plasma membrane vesicles (50 μg of protein) were added to 500 μL of a buffer containing 10 mM MES–Tris (pH 6.0), 330 mM sucrose, 140 mM KCl, 4 mM $MgCl_2$, 0.1 mM EDTA, 1 mM DTT, 50 mM KNO_3, 1 mM NaN_3, 0.1 mM Na_2MoO_4, and 5 μM acridine orange. Proton translocation was initiated in vesicles by the addition of 2 mM ATP. The dissipation of acridine orange absorbance was monitored at 495 nm using Beckman DU640 spectrophotometer. The ATP-dependent H^+-transport activity was inhibited after 3 min by the addition of 0.5 mM sodium orthovanadate. As(III) was then added to the final 10 mM concentration and increase in the rate of acridine orange absorbance (i.e. decay of the pH gradient) was used for measurements of As(III)-dependent dissipation of the preformed, inside-acid pH gradient.

3. Results

3.1. Mutagenesis of cysteine residues in Acr3p permease

It has been proposed that a single cysteine residue in the *C. glutamicum* (Cys129) and *A. metalliredigens* (Cys138) Acr3 transporters is required for arsenite efflux [11,25]. In contrast to prokaryotic members of Acr3 family, the *S. cerevisiae* Acr3 protein sequence is particularly rich in cysteine residues (nine in total) which are predicted to localize in transmembrane segments (TM) and intracellular loops (Fig. 1B). Cys151, which is conserved in all Acr3 proteins identified so far (Fig. 1A), is predicted to localize in the middle of TM4 (Fig. 1B) similarly to bacterial Acr3 transporters [11,17,25]. Interestingly, two cysteines (Cys90 and Cys169) are localized in the cytosolic loops but in close proximity to transmembrane regions, which are conserved in the majority of eukaryotic members of the Acr3 family (Fig. 1A). The remaining six cysteine residues are found only in yeasts (Saccharomycotina) and predicted to

localize either in transmembrane segments (Cys192, TM5; Cys283, TM8; Cys344, TM9) or in a big intracellular loop connecting TM8 and TM9 (Cys316, Cys318, Cys333) (Fig. 1B). To examine the role of cysteine residues in metalloid transport via the *S. cerevisiae* Acr3p, each cysteine residue was replaced with alanine or valine by site-directed mutagenesis using the centromeric plasmid containing the *ACR3* gene fused to GFP (pACR3-GFP) as a template. The resulting plasmids bearing mutant variants of *ACR3* gene, the wild-type *ACR3* plasmid and an empty vector were introduced to the yeast *acr3* deletion mutant (*acr3*Δ) by transformation for further phenotypic characterization.

3.2. Functional analysis of Acr3p mutants

First, we tested the ability of Acr3p cysteine mutants to complement high-level sensitivity to As(III) and As(V) and moderate sensitivity to Sb(III) in the *acr3*Δ mutant (Fig. 2A). The C151V mutant did not confer any resistance to all tested metalloids suggesting that this mutation leads to a complete loss of Acr3p function. Expression of C90A and C169A mutants conferred residual resistance to metalloids in *acr3*Δ cells. The C283A mutant behaved like the wild-type Acr3p, while replacement of Cys192, Cys316, Cys318, Cys333 and Cys344 to alanines resulted in a slight reduction of growth in the presence of high concentrations of As(III). To better assess functionality of Acr3p cysteine mutants, the *acr3*Δ transformants were cultivated in liquid medium containing 1 mM As(III) for 32 h (Fig. 2B). Consistently, the C90A, C151V, and C169A transformants showed no growth in the presence of 1 mM As(III), while growth of the C283A mutant was similar to wild-type strain. Expression of C192A, C316A, C318A, C333A and C344A conferred residual or intermediate resistance to 1 mM As(III).

To check whether the observed growth defects in the presence of metalloids are a result of impairment of Acr3p ability to extrude As(III), we measured As(III) efflux from the *acr3*Δ cells expressing Acr3p cysteine mutants (Fig. 2C). Cells were incubated with high concentration of As(III) to allow its accumulation within the cells and then released in fresh medium to allow As(III) efflux. The C151V and *acr3*Δ mutants showed negligible decrease of As(III) content suggesting lack of Acr3p-dependent extrusion of As(III) out of the cells. All remaining cysteine mutants with the exception of C283A also displayed reduction of As(III) efflux compared to the cells expressing the wild-type Acr3p. We conclude that mutagenesis of any cysteine residue in the *S. cerevisiae* Acr3p apart from Cys283 leads to either loss or significant reduction of As(III) transport. Based on these results, we classified the C151V mutant as non-functional, C90A, C169A, C192A, C316A, C318A, C333A and C344A mutants as partially functional and the C283A mutant as functional (Table 1).

3.3. Cys90 is required for Acr3p trafficking from the ER to the plasma membrane

Loss of Acr3 function due to cysteine mutagenesis might be a result of decreased protein stability, improper trafficking to the plasma membrane and/or impairment of transport activity. First, we checked expression of Acr3p variants after As(III) induction at the level of transcription and found that wild-type and mutated Acr3p showed similar mRNA levels (Fig. 3A). Consistently, we detected equivalent amounts of wild-type and mutated Acr3 proteins in total protein extracts suggesting that mutagenesis of cysteines does not lead to decreased stability or improper overall folding of Acr3p variants (Fig. 3B). Finally, the subcellular

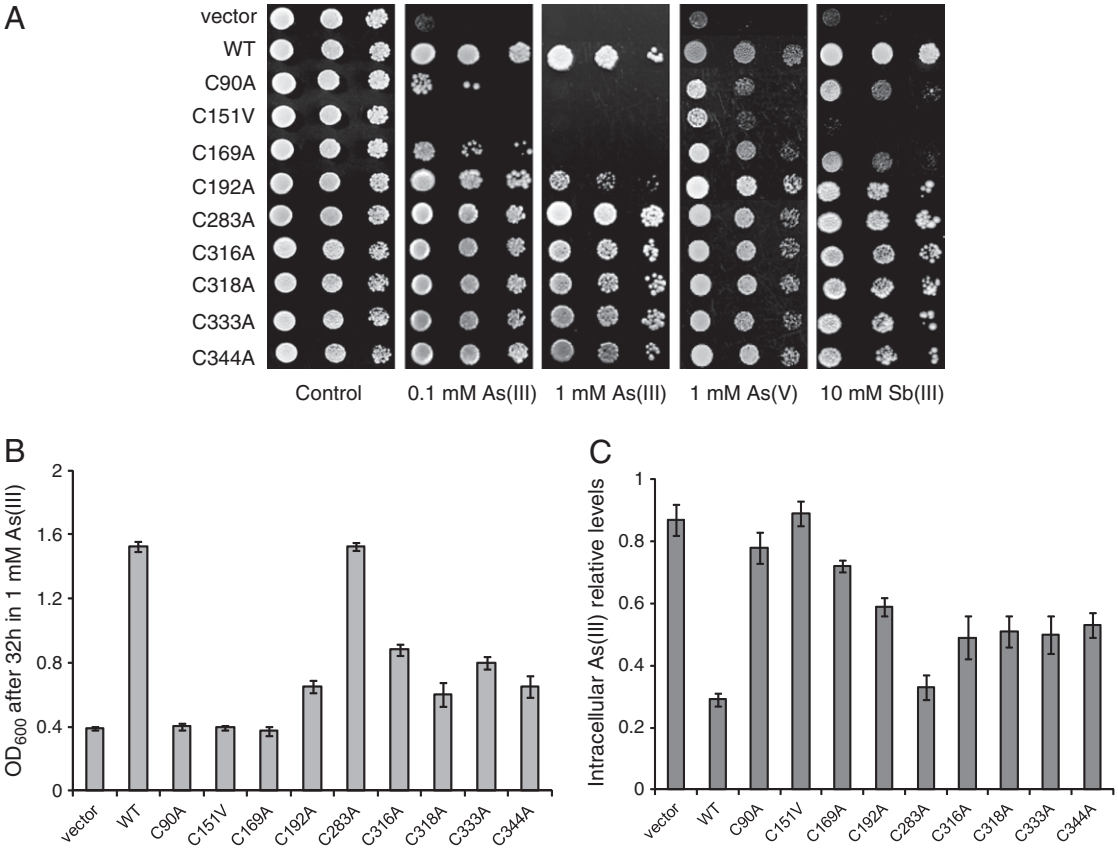

Fig. 2. Resistance to metalloids and arsenite content in cells expressing the Acr3p cysteine mutants. (A) Cultures of *acr3*Δ cells bearing control vector or expressing wild-type Acr3p (WT) or Acr3p cysteine mutants were serially diluted and spotted on selective minimal solid media containing various concentrations of arsenite (As(III)), arsenate (As(V)) and antimonyl potassium tartrate (Sb(III)). Plates were photographed after 3 days at 30 °C. (B) The indicated *acr3*Δ transformants were cultivated in liquid minimal media in the presence of 1 mM As(III) for 32 h at 30 °C before measuring optical density at 600 nm. In a control experiment without As(III) all transformants showed similar growth rate (not shown). (C) As(III) efflux was determined in the *acr3*Δ transformants as described in the Materials and methods. Error bars indicate the standard deviations of three assays.

Table 1
Summary of phenotypic analysis of Acr3p cysteine mutants.

Acr3p version	Mutated region	Complementation of As(III) sensitivity	Subcellular localization	Transport activity	Mutant class
Wild type	None	+++	PM	+++	F
C90A	L2	+	PM + ER	+	PF
C151V	TM4	−	PM	−	NF
C169A	L4	+	PM + ER	+	PF
C192A	TM5	++	PM	++	PF
C283A	TM8	+++	PM	+++	F
C316A	L8	++	PM	++	PF
C318A	L8	++	PM + PS	++	PF
C333A	L8	++	PM + PS	++	PF
C344A	TM9	++	PM + ER	++	PF

Mutated region: L2, L4, and L8 — intracellular loops; TM4, TM5, TM8, and TM9 — transmembrane spans. Complementation of As(III) sensitivity and transport activity: − none; ++ partial, and +++ full. Subcellular localization: PM — plasma membrane, ER — endoplasmic reticulum, and PS — punctate structures. Mutant class: F — functional, PF — partially functional, and NF — non-functional.

localization of Acr3-GFP proteins was determined by fluorescence microscopy (Fig. 3C). The wild-type Acr3p-GFP, C151V, C192A, C283A and C316A mutants were present at the cell surface confirming their proper localization at the plasma membrane. C169A and C344A showed strong continuous signal at the cell surface as well as weaker intracellular signal in the form of ring around the nucleus (Fig. 3C and data not shown) resembling the nuclear endoplasmic reticulum (ER) [31,32]. This suggests that although C169A and C344A exhibit some exit delay from the ER, they accumulate at the plasma membrane at high levels. The C90A mutant showed a typical localization for ER-trapped proteins, i.e. continuous or discontinuous fluorescence signal was present at the intracellular membranes around the nucleus (the nuclear ER), at the cell surface (the cortical or peripheral ER underlying the plasma membrane) and in the cytoplasm (ER connecting tubules) [31,33]. C318A and C333A were found both at the plasma membrane and in punctate structures dispersed in the cytoplasm that may correspond to the Golgi/endosomal network [31,34]. Considering trafficking perturbations observed for some Acr3p mutants (C90A, C169A, C318A, C333A, C344A), plasma membrane vesicles were isolated, followed by immunoblotting with anti-GFP to compare levels of Acr3p-GFP variants in the plasma membrane and anti-Pma1p as loading and membrane fraction quality controls (Fig. 3D). Consistent with the fluorescence microscopy data, the C90A mutant protein was hardly detectable in the plasma membrane fraction indicating that Cys90 is required for efficient sorting of Acr3p from the ER to the plasma membrane. Importantly, the wild-

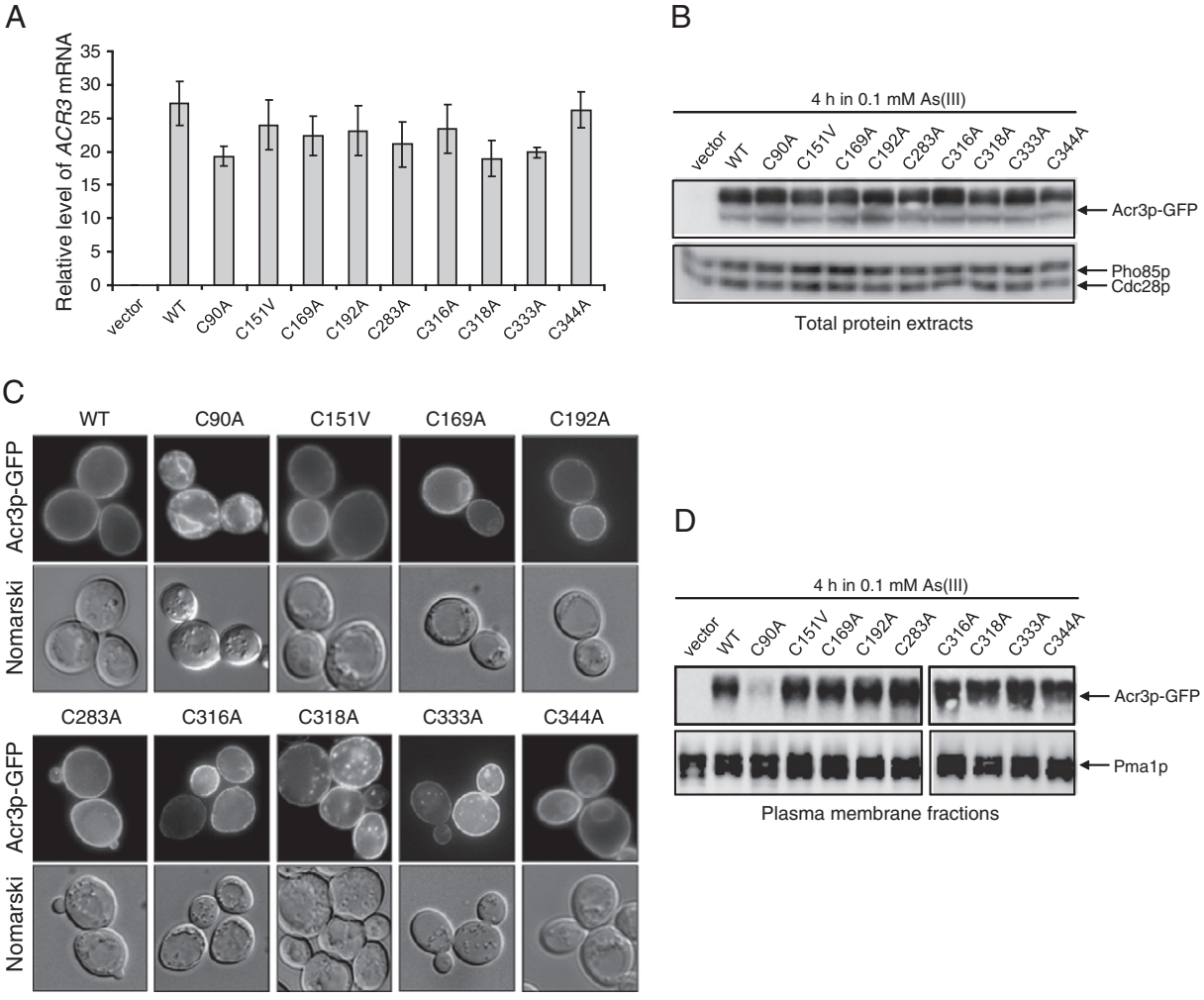

Fig. 3. Expression and subcellular localization of Acr3p mutant variants. (A) Transcription of *ACR3* mutant genes. Total RNA was isolated from the indicated *acr3*Δ transformants after exposure to 0.1 mM As(III) for 4 h and assayed by quantitative PCR. Error bars indicate the standard deviations of three independent experiments. (B) Western blot analysis of total protein extracts prepared from the *acr3*Δ cells expressing mutant variants of Acr3p after 4 h incubation in the presence of 0.1 mM As(III). Blots were probed with the anti-GFP antibody to detect Acr3p-GFP and the anti-PSTAIRE antibody to detect cyclin-dependent kinases Cdc28p and Pho85p as loading controls. (C) Samples from cultures analyzed in (A) and (C) were also examined by fluorescence microscopy to visualize subcellular localization of Acr3p-GFP mutants. (D) Immunodetection of Acr3p-GFP and Pma1p in the membrane vesicles prepared from the *acr3*Δ yeast cells expressing mutant variants of Acr3p. Blots were probed with the anti-GFP antibody to detect Acr3p-GFP and the anti-Pma1p antibody as a loading and plasma membrane quality control.

type Acr3 and remaining eight cysteine mutants displayed high protein levels at the plasma membrane. Thus, mutagenesis of Cys151, Cys169, Cys192, Cys316, Cys318, Cys333 and Cys344 residues may directly impair transport activity of the Acr3p permease.

The above results show that Cys90 is required for the Acr3p exit from the ER to the plasma membrane (Fig. 3). Cys90 is predicted to localize in the cytoplasmatic loop close to TM2 (Fig. 1B) and may be the site of S-palmitoylation. Addition of palmitate, a C16 saturated fatty acid, to cysteine residue may initiate conformation changes of adjacent transmembrane helix by tilting it within the membrane to gain a proper folding and assembly of whole membrane protein [35,36]. Retention of palmitoylation-deficient proteins in the ER may be a result of unmasking neighboring lysine which then can be ubiquitinated as it has been reported for the mammalian lipoprotein receptor-related protein 6 (LRP6) [37]. Interestingly, it could be the case for Cys90 which precedes Lys91 in Acr3p (Fig. 1B). To test this hypothesis, Lys91 was replaced with Arg in wild type Acr3p and the C90A variant and the resulting mutants were analyzed for its ability to localize in the plasma membrane and confer metalloid resistance (Fig. 4). The single K91R mutant showed wild type phenotype, while the double C90A,K91R mutation led to full recovery of Acr3p function. Compared to the C90A variant, the double C90A,K91R mutant was no longer trapped in ER and accumulated in the plasma membrane (Fig. 4B and C). Importantly, the Acr3p mutant lacking a potential S-palmitoylation site, properly, targeted to the plasma membrane exhibited full activity as the double C90A,K91R mutant complemented metalloid sensitivity of *acr3*Δ cells (Fig. 4D). This indicates that Cys90 may be subjected to S-palmitoylation to prevent ubiquitination of neighboring Lys91 which leads to retention of the protein in the ER as a part of membrane protein quality system [36,37].

3.4. Involvement of cysteines in Acr3p-mediated As(III) transport

The role of cysteine residues in Acr3p transport activity was further confirmed by detailed transport assays using plasma membrane vesicles (Fig. 5). Previous studies on the kinetic properties of Acr3p-mediated As(III) efflux revealed that Acr3p acts as a trivalent metalloid/H^+ antiporter with the apparent K_m of 2 mM for As(III) and

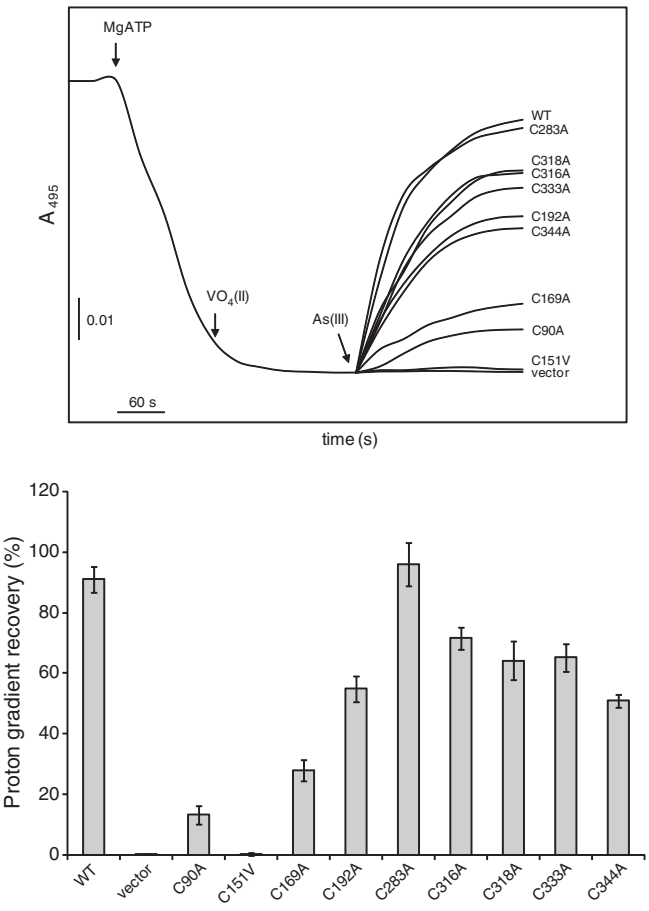

Fig. 5. Arsenite-dependent H^+ transport across everted plasma membrane vesicles. Preparation of everted plasma membrane vesicles and measurement details of H^+/As(III) antiport activity were described in the Materials and methods. 10 mM As(III) was used to dissipate the pH gradient across the vesicles. Error bars indicate the standard deviations of three assays.

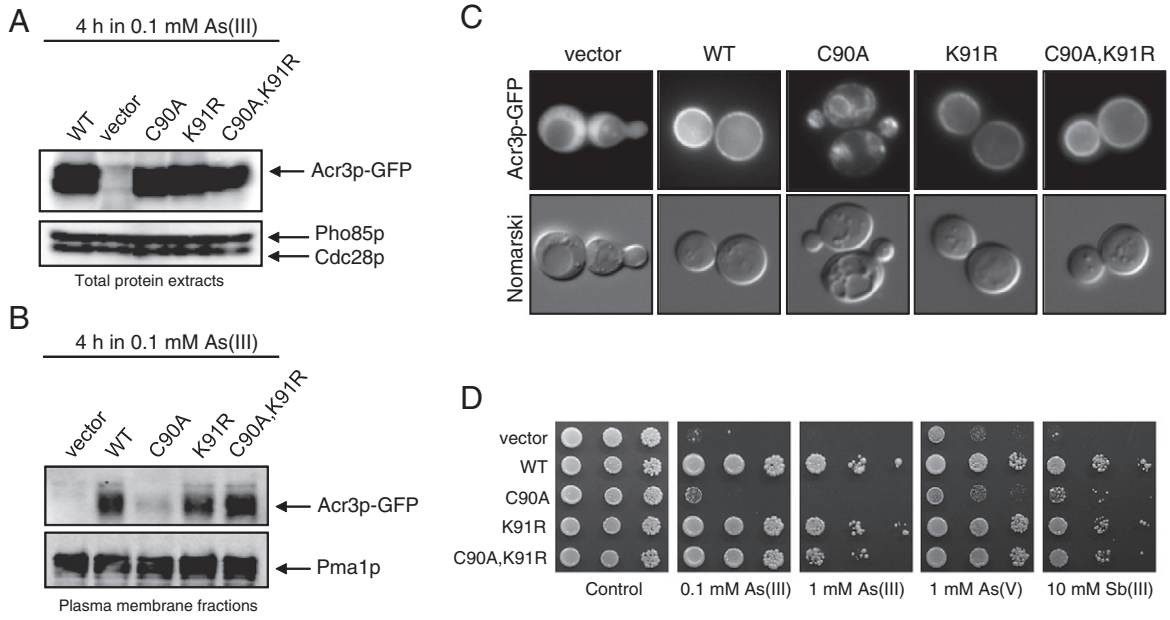

Fig. 4. ER retention of the Acr3 mutant protein lacking Cys90 requires Lys91. Western blot analysis of total protein extracts (A) and the plasma membrane-enriched fractions (B) prepared from the *acr3*Δ cells bearing control vector or expressing wild-type Acr3p (WT) or indicated Acr3p mutants. (C) Subcellular localization of Acr3p-GFP mutants was analyzed by fluorescence microscopy. (D) Cultures of indicated *acr3*Δ transformants were serially diluted and spotted on selective minimal solid media containing various concentrations of arsenite (As(III)), arsenate (As(V)) and antimonyl potassium tartrate (Sb(III)). Plates were photographed after 2 days at 30 °C.

Sb(III) [24]. It has been shown that the full recovery of proton gradient generated by Pma1p in the plasma membranes isolated from the Acr3p-expressing yeast cells was observed at 5–10 mM As(III) in a reaction mixture [24]. Therefore, to examine whether cysteine residues are required for Acr3p transport activity, the rate of gradient recovery in ΔpH energized vesicles was studied following the addition of 10 mM As(III) into the transport assay. In agreement with our previous study [24], the wild-type Acr3p utilized over 90% of proton gradient preformed by ATP-dependent Pma1p proton pump to transport As(III) across the plasma membranes (Fig. 5). Mutagenesis of Cys151, that is conserved in all members of Acr3 family, resulted in a complete loss of transport activity indicating that Cys151 plays a crucial role in Acr3p transport function (Fig. 5). Residual Acr3p activity in the plasma membranes isolated from the C90A mutant was consistent with the results of western blot analysis and fluorescence imaging revealing that this mutation impairs secretion of Acr3p to the plasma membrane, and thus negatively affects As(III) efflux. Mutagenesis of Cys283 did not alter the Acr3p-mediated As(III)/H^+ exchange across the everted plasma membrane vesicles confirming that this residue is not essential for Acr3p function (Fig. 5). Conversely, substitutions of Cys169, Cys192, Cys316, Cys318, Cys333 and Cys344 with alanines resulted in a partial impairment of Acr3p transport properties (Fig. 5). However, the rate of Acr3p-mediated As(III)/H^+ exchange in plasma membrane vesicles isolated from these mutants was differentially reduced by 30–40% for C316A, C318A and C333A mutants, 50% for C192A and C344A mutants and even by 70% for the C169A mutant when compared to native Acr3p activity (Fig. 5).

Our data suggest that the C151V mutant lacks transport activity, while the remaining seven cysteine mutants possess reduced ability to extrude As(III) due to very low protein level at the plasma membrane (C90A) or decreased rate of As(III) translocation (Cys169, Cys192, Cys316, Cys318, Cys333 and Cys344) (Table 1). Based on the assumption that overexpression of partially functional proteins, but not catalytically inactive variant, should compensate trafficking perturbations or reduced efflux rate, we expressed the mutated *ACR3* genes under control of the strong *MET25* promoter on a plasmid and checked complementation of As(III) hypersensitivity in the *acr3*Δ mutant (Fig. 6). Indeed, overexpression of all cysteine mutants, with the exception of C151V, conferred resistance to metalloids at a wild-type level. In contrast, *acr3*Δ cells overexpressing the C151V mutant remained highly sensitive to metalloids, confirming the absolute requirement of Cys151 for metalloid transport via the Acr3p permease. Interestingly, compared to the *acr3*Δ mutant bearing a control vector expression of the C151V variant conferred some resistance to As(V) (Figs. 1A and 6). This may suggest that As(III) formed after As(V) reduction by the arsenate reductase Acr2p leaks out of the cell through the Acr3p lacking Cys151 down the concentration gradient as it has been shown for the aquaglyceroporin Fps1p [38]. Thus, it is tempting to speculate that Cys151 is a major determinant of transport features of Acr3p including metalloid/H^+ exchange activity, selectivity towards As(III) and Sb(III) and permeability barrier.

4. Discussion

The Acr3p permease from the yeast *S. cerevisiae* is a prototype member of Acr3 family of transporters, which are found in all domains of life [8–10] (Fig. 1A). It has been recently determined that both bacterial and yeast Acr3 permeases act as As(III)/H^+ antiporters [24,25]. Interestingly, the *C. glutamicum* Acr3 is specific for As(III) (11,25), while the *S. cerevisiae* Acr3p is also able to transport Sb(III) [21,24]. However, there are no structural data for Acr3 proteins which could suggest mechanisms of substrate specificity or metalloid translocation.

It has been revealed that a single cysteine residue in the *C. glutamicum* (Cys129) and *A. metalliredigens* Acr3 (Cys138) is indispensable for As(III) efflux [11,25]. Mutagenesis of the remaining cysteine residues in the *C. glutamicum* Acr3 (Cys141) and the *A. metalliredigens* Acr3 (Cys27, Cys91) had little effect on As(III) transport properties [11]. Importantly, both Cys129 (*C. glutamicum*) and Cys138 (*A. metalliredigens*) are located in the middle of transmembrane domain and conserved in all members of the Acr3 family leading to the hypothesis that a single cysteine residue may serve as a selectivity barrier allowing As(III) translocation due to low affinity binding to a thiol group [11,25]. Mutagenesis scanning of conserved hydrophilic residues, which are predicted to localize in transmembrane domains of *C. glutamicum* Acr3, showed that Glu305 is also essential for As(III) transport activity [25]. It has been hypothesized that Glu305 together with Cys129 constitutes a selectivity filter for As(III) or participates in proton translocation [25].

Here, we report the phenotypic analysis of nine cysteine mutations in the *S. cerevisiae* Acr3p. In agreement with previous data obtained for bacterial Acr3 transporters [11,25], we found that the highly conserved Cys151 is indispensable for the As(III)/H^+ antiport mediated by the yeast Acr3p (Figs. 2 and 5). Thus, both prokaryotic and eukaryotic members of the Acr3 family of transporters share similar mechanism of As(III) translocation with a catalytic-active role of the single cysteine residue localized in the middle of TM4.

However, Acr3 orthologs from eukaryotes are characterized by the presence of two additional highly conserved cysteine residues, Cys90 and Cys169 in the yeast Acr3p (Fig. 1A). Importantly, C90A and C169A

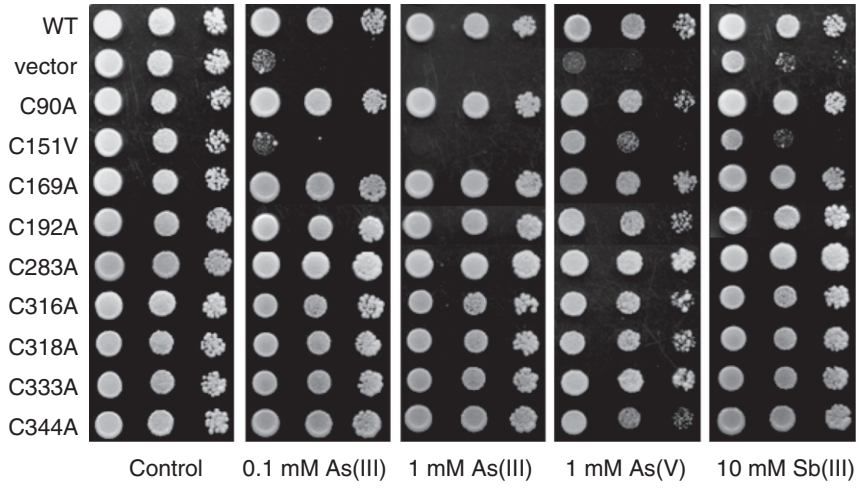

Fig. 6. The effect of overexpression of Acr3p cysteine mutants on the level of metalloid resistance. The *acr3*Δ cells expressing mutant variants of *ACR3* gene under the control of strong and constitutive *MET25* promoter were serially diluted and spotted on selective minimal solid media in the presence of arsenite (As(III)), arsenate (As(V)) and antimonyl potassium tartrate (Sb(III)). Plates were photographed after 2 days at 30 °C.

substitutions strongly impaired Acr3p function, although probably by different mechanisms. Subcellular localization studies revealed that Cys90 is required for Acr3p sorting from the ER to the plasma membrane (Figs. 3 and 4). Since Cys90 resides within the cytosolic loop in the proximity of the transmembrane domain (Fig. 1B), we hypothesize that Cys90 may be subjected to S-palmitoylation to ensure proper folding and assembly of Acr3p before the ER exit. It has been observed that the ER export of the yeast chitin synthase Chs3p, which contains six to eight transmembrane spans and localizes to the plasma membrane, requires S-palmitoylation mediated by the protein acyl transferase Pfa4p [39]. This post-translation modification prevents Chs3p from aggregation into high-molecular mass complexes and may be a general regulatory mechanism of polytopic transmembrane protein folding and sorting [39]. Indeed, global search for protein palmitoylation in yeast revealed that twelve amino acid permeases are subjected to S-palmitoylation [40]. It has been also shown that in the absence S-palmitoylation the retention of mammalian signaling protein LPR6 in the ER requires monoubiquitination without premature degradation [37]. On the other hand, the yeast SNARE Tlg1 lacking S-palmitoylation undergoes ubiquitination that targets the protein for degradation in the vacuole [41]. This suggests the existence of conserved mechanism of ubiquitin-dependent quality control system which is inhibited by palmitoylation as a marker of properly folded and assembled membrane proteins which are ready to exit the ER [37,39,41]. Similarly to LPR6, the retention of Acr3p mutant lacking Cys90 in the ER was rescued by replacing the neighboring Lys91 with Arg (Fig. 4B and C) and the C90A,K91R mutant properly localized in the plasma membrane conferred wild type level of metalloid resistance (Fig. 4D). In the future it will be interesting to investigate whether Cys90 and Lys91 in Acr3p are indeed subjected to palmitoylation and ubiquitination, respectively, to regulate Acr3p targeting to the plasma membrane.

In contrast to Cys90 mutagenesis, the C169A mutant, which is also characterized by the strong defect in As(III) efflux, displayed only a minor exit delay from the ER (Fig. 3C) and was present in the plasma membrane at the level comparable to the wild-type Acr3p (Fig. 3D). Cys169 is localized in the vicinity of TM5 (Fig. 1B) and thus it is tempted to speculate that this residue may be involved in As(III) binding and directing it to the translocation pore of Acr3p. The remaining three cysteines (Cys316, Cys318 and Cys333), which all reside in the cytosolic loop connecting TM8 and TM9 (Fig. 1B), may play a similar role. However, such large loop is present only in the Acr3 proteins from yeast species (Fig. 1A) and substitutions of Cys318 and Cys333 with alanines not only moderately reduced As(III) transport (Fig. 5) but also impaired Acr3p trafficking (Fig. 3C). Hence, it is difficult to assess the functional significance of these cysteine residues in Acr3p.

In addition to Cys151, the *S. cerevisiae* Acr3p contains three more cysteines (Cys192, Cys283, Cys344) predicted to localize in various transmembrane segments (Fig. 1B). Mutagenesis of Cys192 and Cys344 resulted in about 50% decrease of Acr3p transport activity (Fig. 5). Acr3p mutants lacking Cys192 and Cys344 may not have sufficient flexibility to allow proper orientation of transmembrane domains in the bilayer. On the other hand, these residues may participate directly in As(III) translocation. The recent theoretical study of the optimal $As(OH)_3$–$(H_2O)_n$ complexes suggests that the arsenic part is very hydrophobic, while the $(OH)_3$ part is very hydrophilic, in which at least two OH groups participate in forming hydrogen bonds with three water molecules [42]. Such amphipathic character of $As(OH)_3$–$(H_2O)_3$ complex with one free OH group that is able to bind to a single thiol group of cysteine with low affinity would allow As(III) movement through Acr3p.

In sum, this study describes the first mutational analysis of eukaryotic arsenite permease Acr3 showing the significant role of multiple cysteine residues in Acr3p-mediated As(III) efflux. Future studies should be aimed at identification of other hydrophilic amino acid residues in Acr3p which are responsible for transport selectivity and the As(III)/H^+ exchange mechanism. It will be of interest to test whether multiple cysteines in other eukaryotic members of the Acr3 family are also important for As(III) transport and trafficking of the proteins to the plasma membrane.

Supplementary data to this article can be found online at http://dx.doi.org/10.1016/j.bbamem.2013.11.013.

Acknowledgements

We greatly appreciate the gift of the anti-Pma1p antibody from Dr. M. Ghislain (Université Catholique de Louvain, Louvain-la-Neuve, Belgium) and the pUG35 plasmid from J.H. Hegemann (Heinrich-Heine-University, Düsseldorf, Germany). This work was supported by grants N301049339 and 1068/S/IBR/2013 from the Polish Ministry of Science and Higher Education.

References

[1] K.S. Smith, H.L.O. Huyck, An overview of the abundance, relative mobility, bioavailability, and human toxicity of metals, in: G.S. Plumlee, M.J. Logsdon (Eds.), The environmental geochemistry of mineral deposits, Part A: Society of Economic Geologists, Reviews in Economic Geology, 1999, pp. 29–70.
[2] D.K. Nordstrom, Worldwide occurrences of arsenic in ground water, Science 296 (2002) 2143–2145.
[3] S. Tapio, B. Grosche, Arsenic in the etiology of cancer, Mutat. Res. 612 (2006) 215–246.
[4] P.J. Dilda, P.J. Hogg, Arsenical-based cancer drugs, Cancer Treat. Rev. 33 (2007) 542–564.
[5] R.W. Ahn, F. Chen, H. Chen, S.T. Stern, J.D. Clogston, A.K. Patri, M.R. Raja, E.P. Swindell, V. Parimi, V.L. Cryns, T.V. O'Halloran, A novel nanoparticulate formulation of arsenic trioxide with enhanced therapeutic efficacy in a murine model of breast cancer, Clin. Cancer Res. 16 (2010) 3607–3617.
[6] P. Bobe, D. Bonardelle, K. Benihoud, P. Opolon, M.K. Chelbi-Alix, Arsenic trioxide: a promising novel therapeutic agent for lymphoproliferative and autoimmune syndromes in MRL/lpr mice, Blood 108 (2006) 3967–3975.
[7] N. Singh, M. Kumar, R.K. Singh, Leishmaniasis: current status of available drugs and new potential drug targets, Asian Pac. J. Trop. Med. 5 (2012) 485–497.
[8] N.M. Mansour, M. Sawhney, D.G. Tamang, C. Vogl, M.H. Saier Jr., The bile/arsenite/riboflavin transporter (BART) superfamily, FEBS J. 274 (2007) 612–629.
[9] B.P. Rosen, M.J. Tamás, Arsenic transport in prokaryotes and eukaryotic microbes, Adv. Exp. Med. Biol. 679 (2010) 47–55.
[10] E. Maciaszczyk-Dziubinska, D. Wawrzycka, R. Wysocki, Arsenic and antimony transporters in eukaryotes, Int. J. Mol. Sci. 13 (2012) 3527–3548.
[11] H.L. Fu, Y. Meng, E. Ordóñez, A.F. Villadangos, H. Bhattacharjee, J.A. Gil, L.M. Mateos, B.P. Rosen, Properties of arsenite efflux permeases (Acr3) from *Alkaliphilus metalliredigens* and *Corynebacterium glutamicum*, J. Biol. Chem. 284 (2009) 19887–19895.
[12] A.R. Achour, P. Bauda, P. Billard, Diversity of arsenite transporter genes from arsenic-resistant soil bacteria, Res. Microbiol. 158 (2007) 128–137.
[13] E. Maciaszczyk, R. Wysocki, P. Golik, J. Lazowska, S. Ulaszewski, Arsenical resistance genes in *Saccharomyces douglasii* and other yeast species undergo rapid evolution involving genomic rearrangements and duplications, FEMS Yeast Res. 4 (2004) 821–832.
[14] E. Indriolo, G. Na, D. Ellis, D.E. Salt, J.A. Banks, A vacuolar arsenite transporter necessary for arsenic tolerance in the arsenic hyperaccumulating fern *Pteris vittata* is missing in flowering plants, Plant Cell 22 (2010) 2045–2057.
[15] G. Duan, T. Kamiya, S. Ishikawa, T. Arao, T. Fujiwara, Expressing *ScACR3* in rice enhanced arsenite efflux and reduced arsenic accumulation in rice grains, Plant Cell Physiol. 53 (2012) 154–163.
[16] W. Ali, J.C. Isner, S.V. Isayenkov, W. Liu, F.J. Zhao, F.J. Maathuis, Heterologous expression of the yeast arsenite efflux system *ACR3* improves *Arabidopsis thaliana* tolerance to arsenic stress, New Phytol. 194 (2012) 716–723.
[17] E.K. Aaltonen, M. Silow, Transmembrane topology of the Acr3 family arsenite transporter from *Bacillus subtilis*, Biochim. Biophys. Acta 1778 (2008) 963–973.
[18] T. Sato, Y. Kobayashi, The *ars* operon in the *skin* element of *Bacillus subtilis* confers resistance to arsenate and arsenite, J. Bacteriol. 180 (1998) 1655–1661.
[19] R. Wysocki, P. Bobrowicz, S. Ulaszewski, The *Saccharomyces cerevisiae ACR3* gene encodes a putative membrane protein involved in arsenite transport, J. Biol. Chem. 272 (1997) 30061–30066.
[20] M. Ghosh, J. Shen, B.P. Rosen, Pathways of As(III) detoxification in *Saccharomyces cerevisiae*, Proc. Natl. Acad. Sci. U. S. A. 96 (1999) 5001–5006.
[21] E. Maciaszczyk-Dziubinska, D. Wawrzycka, E. Sloma, M. Migocka, R. Wysocki, The yeast permease Acr3p is a dual arsenite and antimonite plasma membrane transporter, Biochim. Biophys. Acta 1798 (2010) 2170–2175.
[22] X. Xia, V.L. Postis, M. Rahman, G.S. Wright, P.C. Roach, S.E. Deacon, J.C. Ingram, P.J. Henderson, J.B. Findlay, S.E. Phillips, M.J. McPherson, S.A. Baldwin, Investigation of the structure and function of a *Shewanella oneidensis* arsenical-resistance family transporter, Mol. Membr. Biol. 25 (2008) 691–705.
[23] L. López-Maury, F.J. Florencio, J.C. Reyes, Arsenic sensing and resistance system in the cyanobacterium *Synechocystis* sp. strain PCC 6803, J. Bacteriol. 185 (2003) 5363–5371.

[24] E. Maciaszczyk-Dziubinska, M. Migocka, R. Wysocki, Acr3p is a plasma membrane transporter that catalyzes As(III)/H^+ and Sb(III)/H^+ exchange in *Saccharomyces cerevisiae*, Biochim. Biophys. Acta 1808 (2011) 1855–1859.
[25] A.F. Villadangos, H.L. Fu, J.A. Gil, J. Messens, B.P. Rosen, L.M. Mateos, Efflux permease CgAcr3-1 of *Corynebacterium glutamicum* is an arsenite-specific antiporter, J. Biol. Chem. 287 (2012) 723–735.
[26] R. Wysocki, C.C. Chéry, D. Wawrzycka, M. Van Hulle, R. Cornelis, J.M. Thevelein, M.J. Tamás, The glycerol channel Fps1p mediates the uptake of arsenite and antimonite in *Saccharomyces cerevisiae*, Mol. Microbiol. 40 (2001) 1391–1401.
[27] A. Delaunay, A.D. Isnard, M.B. Toledano, H_2O_2 sensing through oxidation of the Yap1 transcription factor, EMBO J. 19 (2000) 5157–5166.
[28] B. Norling, Two-phase partitioning as a method for isolation of tight plasma membrane vesicles from *Saccharomyces cerevisiae* and from *Chlamydomonas reinhardtii*, in: R. Hatti-Kaul (Ed.), Methods in Biotechnology, Aqueous Two-phase Systems: Methods and Protocols, 11, Humana Press Inc., Totowa, NJ, 2000, pp. 177–184.
[29] G.E. Tusnády, I. Simon, The HMMTOP transmembrane topology prediction server, Bioinformatics 17 (2001) 849–850.
[30] F. Sievers, A. Wilm, D.G. Dineen, T.J. Gibson, K. Karplus, W. Li, R. Lopez, H. McWilliam, M. Remmert, J. Söding, J.D. Thompson, D. Higgins, Fast, scalable generation of high-quality protein multiple sequence alignments using Clustal Omega, Mol. Syst. Biol. 7 (2011) 539.
[31] M. Lowe, F.A. Barr, Inheritance and biogenesis of organelles in the secretory pathway, Nat. Rev. Mol. Cell Biol. 8 (2007) 429–439.
[32] A. Merhi, N. Gérard, E. Lauwers, M. Prévost, B. André, Systematic mutational analysis of the intracellular regions of yeast Gap1 permease, PLoS One 6 (2011) e18457.
[33] C.L. Young, D.L. Raden, A.S. Robinson, Analysis of ER resident proteins in *Saccharomyces cerevisiae*: implementation of H/KDEL retrieval sequences, Traffic 14 (2013) 366–381.
[34] T. Hachiro, T. Yamamoto, K. Nakano, K. Tanaka, Phospholipid flippases Lem3p-Dnf1p and Lem3p-Dnf2p are involved in the sorting of the tryptophan permease Tat2p in yeast, J. Biol. Chem. 288 (2013) 3594–3608.
[35] J. Greaves, L.H. Chamberlain, Palmitoylation-dependent protein sorting, J. Cell Biol. 176 (2007) 249–254.
[36] S. Blaskovic, M. Blanc, F.G. van der Goot, What does S-palmitoylation do to membrane proteins, FEBS J. 280 (2013) 2766–2774.
[37] L. Abrami, B. Kunz, I. Iacovache, F.G. van der Goot, Palmitoylation and ubiquitination regulate exit of the Wnt signaling protein LRP6 from the endoplasmic reticulum, Proc. Natl. Acad. Sci. U. S. A. 105 (2008) 5384–5389.
[38] E. Maciaszczyk-Dziubinska, I. Migdal, M. Migocka, T. Bocer, R. Wysocki, The yeast aquaglyceroporin Fps1p is a bidirectional arsenite channel, FEBS Lett. 584 (2010) 726–732.
[39] K.K. Lam, M. Davey, B. Sun, A.F. Roth, N.G. Davis, E. Conibear, Palmitoylation by the DHHC protein Pfa4 regulates the ER exit of Chs3, J. Cell Biol. 174 (2006) 19–25.
[40] A.F. Roth, J. Wan, A.O. Bailey, B. Sun, J.A. Kuchar, W.N. Green, B.S. Phinney, J.R. Yates III, N.G. Davis, Global analysis of protein palmitoylation in yeast, Cell 125 (2006) 1003–10013.
[41] J. Valdez-Taubas, H. Pelha, Swf1-dependent palmitoylation of the SNARE Tlg1 prevents its ubiquitination and degradation, EMBO J. 24 (2005) 2524–2532.
[42] A. Ramírez-Solís, M. Ho, J. Hernández-Cobos, I. Ortega-Blake, Theoretical study of the optimal $As(OH)_3$–H_2O complex: interaction energy and topological analysis of the electronic density, Comp. Theor. Chem. 967 (2001) 44–49.